

Plasma-Induced Frequency Chirp of Intense Femtosecond Lasers and Its Role in Shaping High-Order Harmonic Spectral Lines

Jung-Hoon Kim and Chang Hee Nam

Department of Physics and Coherent X-Ray Research Center, Korea Advanced Institute of Science and Technology, Taejeon 305-701, Korea
(October 31, 2018)

We investigate the self-phase modulation of intense femtosecond laser pulses propagating in an ionizing gas and its effects on collective properties of high-order harmonics generated in the medium. Plasmas produced in the medium are shown to induce a positive frequency chirp on the leading edge of the propagating laser pulse, which subsequently drives high harmonics to become positively chirped. In certain parameter regimes, the plasma-induced positive chirp can help to generate sharply peaked high harmonics, by compensating for the dynamically-induced negative chirp that is caused by the steep intensity profile of intense short laser pulses.

42.65.Ky, 52.40.Nk, 32.80.Rm

Recent remarkable progress in high-power femtosecond laser technology has provided a novel opportunity to investigate high-order harmonic generation processes in an unprecedented high-intensity, ultrashort pulse regime. While necessary for generating high-order harmonics with wavelength extremely short compared to the laser wavelength [1,2], the use of lasers in this regime has some other important merits: the harmonic conversion efficiency is dramatically enhanced [3,4], and the harmonic pulse duration can be reduced to a subfemtosecond time scale [5,6].

As the laser pulse evolves into the high-intensity, ultrashort regime, high harmonic emission begins to exhibit complicated spectral features, such as harmonic line broadening, blueshifting, splitting, and smearing [5–10]. All of these features are absent in the high harmonic spectra observed for lasers with weak intensity well below the ionization saturation intensity and long pulse duration (longer than a few hundred femtoseconds) that show well-defined narrow harmonic peaks almost exactly at odd multiples of the fundamental laser frequency. The involved spectral features showing up for intense short laser pulses can be satisfactorily accounted for, at least at the single-atom level, in terms of decomposition of high harmonics into quantum-path components, and different behaviors of the quantum-path components, in laser fields with rapidly-varying instantaneous intensity [10–12].

Since high-intensity laser pulses can ionize atoms producing plasmas that can affect propagating waves, a proper understanding of macroscopic high harmonic structure necessitates a detailed knowledge of the plasma-related propagation effect as well as the single-atom effect. It is known that an increase in electron density during the laser pulse duration causes the refractive index of a medium to decrease with time, which leads to frequency upshifting and spectral broadening of the laser pulse [13–17]. Because the change in the driving laser spectrum should be reflected in the harmonic conversion,

one might expect that harmonic spectral lines would likewise be blueshifted and broadened. In reality, however, the harmonic spectrum exhibits behavior more complicated than this expectation, as demonstrated in this paper. As a matter of fact, there is another source that can affect the harmonic spectral line shape: the dynamically-induced harmonic chirp (dynamic chirp) that is brought about by a steep pulse envelope [11,18]. The observed spectral behavior of high harmonics can only be understood through inspecting the temporal variation of harmonic frequency caused by the plasma-induced change in the laser frequency, in close connection with the dynamic chirp.

In this paper, we elucidate how the plasma effect modulates the spectrum of an intense femtosecond laser pulse, and discuss its subsequent influence and the effect of laser focusing on macroscopic high harmonic spectra. It is shown that the plasmas induce a positive frequency chirp on the leading edge of the laser pulse up to the point at which a maximum blueshift is attained, and a negative chirp on the remaining part of the laser pulse. Depending on the relative amount of the plasma-induced chirp compared to the dynamic chirp, not only broadening but also narrowing can occur in high harmonic spectral lines. We demonstrate these using a one-dimensional (1D) model, in which the atomic response to the laser is calculated from the 1D Schrödinger equation, and propagations of the laser and harmonic fields are considered in 1D space along the propagation axis.

In order to see how the laser field E_1 is affected by the plasmas (whose effects are dominated by electrons) produced in the medium, we begin by finding a solution of the 1D wave equation:

$$\frac{\partial^2 E_1(x, t)}{\partial x^2} - \frac{1}{c^2} \frac{\partial^2 E_1}{\partial t^2} = \frac{\omega_p^2(x, t)}{c^2} E_1, \quad (1)$$

where $\omega_p(x, t) = \omega_0 [N_e(x, t)/N_{cr}]^{1/2}$ is the local plasma frequency, and ω_0 is the laser frequency. The critical

plasma density N_{cr} is given in Gaussian units by $N_{cr} = m_e \omega_0^2 / 4\pi e^2$, where m_e is the electron mass. To calculate the electron density $N_e(x, t)$, we use the ADK model [19], and consider sequential tunneling ionization up to as high stages of ionization as needed, neglecting collisional ionization that is of little significance in the parameter regions in which high harmonic generation experiments are commonly carried out. At the present gas pressures (≤ 100 Torr) much lower than 1 atm, the energy loss and temporal broadening of the laser are negligible [15]; thus, we may ignore the amplitude modulation of the laser field. Assuming the Gaussian incident pulse $E_1(x, t) = E_0 \exp[-(2 \ln 2 / \Delta t^2)(t - x/c)^2 - i\omega_0(t - x/c)]$ that is a solution to Eq. (1) in free space with Δt being the full width at half maximum (FWHM) of the pulse, we may then write the solution of Eq. (1) in the medium as

$$E_1(x, t) = E_0 \exp[-(2 \ln 2 / \Delta t^2)(t - x/c)^2 - i\omega_0 t + i \int^x n(x', t - |x - x'|/c) \frac{\omega_0}{c} dx'], \quad (2)$$

where $n(x, t) = [1 - N_e(x, t)/N_{cr}]^{1/2}$ is the refractive index of the medium. This expression turns out to be a good approximate solution of Eq. (1) under the conditions $N_e/N_{cr} \ll 1$ and $|c^{-1} \int^x (\partial n / \partial t) dx'| \ll 1$, which are satisfied in the parameter regions considered in this paper.

To confirm that Eq. (2) indeed closely approximates the exact solution, we present in Fig. 1 some typical spectra of 30-fs laser pulses at the exit of the medium (Ne gas) calculated from Eq. (2), along with those obtained from direct numerical calculations of Eq. (1). Use of the explicit expression in Eq. (2) of course significantly reduces the computational time. Upon comparison, it is obvious that the approximate solutions presented in Fig. 1(a) agree well with the exact numerical results in Fig. 1(b) in the parameter regions considered. It can be seen that, as the gas density increases and/or as the laser intensity increases, the spectrum shifts toward a higher-frequency region and becomes broader.

More detailed features of the laser pulse passing through the medium can be revealed with the help of the Wigner distribution function [18], that allows a view of temporal variation of the laser spectrum. The Wigner distributions, calculated under the same conditions as in Fig. 1, are displayed in Fig. 2. It can be observed that, owing to the phase modulation induced by plasmas produced in the medium, the laser frequency increases with time (becomes positively chirped) in the leading edge, and then decreases (becomes negatively chirped) back to the original frequency in the remaining part of the pulse. We note that at the moment when the plasma-induced chirp changes sign from positive to negative, the production rate of electrons reaches its maximum. This moment, at which the laser experiences a maximum blueshift, comes earlier in time as the laser intensity in-

creases, as can be seen from Fig. 2.

When focused laser beams are used, as in usual high harmonic generation experiments, due regard should also be paid to the focusing effect that can change the amplitude and phase of the laser field. In fact, in three-dimensional (3D) simulations this focusing effect could have been automatically considered. Apparently, however, the 1D wave equation in Eq. (1) cannot deal with this effect. Nevertheless, via Eq. (2) the focusing effect can be taken into account along the propagation axis as follows:

$$E_{1f}(x, t) = E_1(x, t)f(x) \exp[i\Phi_f(x)], \quad (3)$$

where $f(x) = [1 + 4(x/b)^2]^{-1/2}$ and $\Phi_f(x) = -\tan^{-1}(2x/b)$ represent, respectively, the amplitude and phase changes due to the focusing [20], and b is the confocal parameter. The laser field given in the form of Eq. (3) now suitably describes the phase modulation induced by plasmas and the focusing effect along the axis, and can be used for discussing the phase matching issue of high harmonics generated *on the propagation axis*.

We next discuss the propagation of high harmonic fields. Since the change in the refractive index in the presence of plasmas is much smaller for higher-frequency waves, we may ignore here the plasma effect. Then the Green function method enables us to write a solution of the 3D wave equation $\nabla^2 E_h - c^{-2}(\partial^2 E_h / \partial t^2) = 4\pi c^{-2}(\partial^2 P / \partial t^2)$ in the following integral form:

$$E_h(\mathbf{r}, t) = - \int \frac{1}{c^2 |\mathbf{r} - \mathbf{r}'|} \frac{\partial^2 P(\mathbf{r}', t')}{\partial t'^2} d^3 r', \quad (4)$$

where t' is the retarded time defined by $t' = t - |\mathbf{r} - \mathbf{r}'|/c$, and the laser-induced polarization P is given in terms of the gas density N_0 and the atomic dipole moment d by $P(\mathbf{r}', t') = N_0 d(\mathbf{r}', t')$. Equation (4) clearly indicates that the harmonic field E_h at t is determined by the coherent sum of the dipole accelerations of atoms in the medium calculated at the retarded time t' .

In our 1D calculations, a medium lies on the propagation axis, and the integration in Eq. (4) is performed in practice over the 1D space along the axis. The medium, a Ne gas of length $l = 700 \mu\text{m}$ at $\simeq 28$ Torr, is uniformly discretized by 200 points, and at each point the dipole acceleration is calculated by numerically solving the 1D Schrödinger equation for an atom in the laser field E_{1f} given in Eq. (3), with $\Delta t = 30$ fs, $\lambda = 800$ nm, $b = 4$ mm, and $I = 1 \times 10^{15}$ W/cm² at the entrance of the medium. After suitably weighted by a constant factor to yield the correct gas density, the results are then added according to Eq. (4) to give E_h .

The high harmonic spectrum calculated in the above way is presented in Fig. 3, which shows the respective roles played by the laser focusing and plasmas in the formation of macroscopic harmonic fields. In Fig. 3(b), we neglect the plasma effect by setting $n(x, t) = 1$ to

concentrate only on the focusing effect. Both the focusing and plasma effects are fully considered in Fig. 3(c), and for comparison we present in Fig. 3(a) a single-atom spectrum calculated for an atom located at the entrance of the medium. Whereas the single-atom spectrum in Fig. 3(a) is smeared with a complicated structure in the plateau region, the macroscopic harmonic spectrum in Fig. 3(b) exhibits discrete harmonic peaks. This is because the intensity-sensitive harmonic components (the long quantum-path component and multiple-recollision components), which give rise to the complicated structure, are suppressed due to their poor phase-matching conditions, leaving only the short quantum-path component [10,21]. Here we emphasize that the variation in the laser intensity caused by the focusing as represented by $f^2(x)$ is mainly responsible for this cleaning up of the harmonic spectrum. At very low gas densities, we may observe a harmonic spectrum similar to that shown in Fig. 3(b). However, at the gas density used in Fig. 3(c), a further change in the harmonic spectrum is caused by the plasma effect: harmonics of low order (43rd and below) undergo spectral broadening, while higher-order harmonics get sharpened.

The plasma-induced harmonic line broadening and narrowing are detailed in Figs. 4 and 5, respectively. The mechanism that shapes high harmonic lines can be explained by making a comparison between the plasma-induced chirp and the dynamically-induced chirp [5,11,18]. Considering that only the leading edge of the laser pulse, where the depletion of neutral atoms is not severe and the electron density is low, is important for the phase-matched harmonic generation, we focus only on this part of the laser pulse. The leading edge of the laser pulse, in which the laser frequency increases with time due to the plasma effect (Fig. 2), tends to generate positively chirped high harmonics. This effect is opposed by the dynamic single-atom effect that, in the present case, forces high harmonics to become negatively chirped [22]. Depending on system parameters and harmonic order, one effect matches or dominates over the other. For instance, for the low-order harmonics in Fig. 4, the dynamic negative chirp is very small [Fig. 4(b)], and the plasma effect dominantly affects the time-frequency characteristics of high harmonics in such a way as to make high harmonics become positively chirped [Fig. 4(d)], leading to spectral line broadening [Fig. 4(c)]. In contrast, the dynamic negative chirp of higher-order harmonics in Fig. 5(b) is substantially large, and the plasma-induced positive chirp more or less cancels out the dynamic chirp [Fig. 5(d)], resulting in harmonic line narrowing [Fig. 5(c)]. In both cases of Figs. 4 and 5, the plasma effect blueshifts the central frequencies of high harmonics.

In conclusion, we have investigated the plasma-induced phase modulation of intense femtosecond laser pulses and its effects on macroscopic high harmonic spectra, using a simple but accurate 1D model. It has been shown that

the plasmas produced in the medium induce a positive frequency chirp on the leading edge of the laser pulses. Strikingly, the plasma-induced chirp, which broadens the laser spectrum, can lead not only to broadening but also to narrowing of harmonic spectral lines. The underlying mechanism has been explained by comparing the plasma-induced positive chirp with the dynamically-induced negative chirp. In stark contrast to the widely reported finding (in regimes well below saturation) that high harmonics are negatively chirped [21,23,24], this study clearly demonstrates that, under laser fields of high intensity and gas pressures not too low, high harmonics can become free of chirp, or even become positively chirped, thanks to the plasma effect. This suggests a way to control the chirp and spectral line shape of high harmonics using the plasma effect.

This work was supported by the Ministry of Science and Technology of Korea through the Creative Research Initiative Program.

-
- [1] C. Spielmann, N. H. Burnett, S. Sartania, R. Koppitsch, M. Schnürer, C. Kan, M. Lenzner, P. Wobrauschek, and K. C. Kulander, *Science* **278**, 661 (1997).
 - [2] Z. Chang, A. Rundquist, H. Wang, M. M. Murnane, and H. C. Kapteyn, *Phys. Rev. Lett.* **79**, 2967 (1997).
 - [3] C. Kan, N. H. Burnett, C. E. Capjack, and R. Rankin, *Phys. Rev. Lett.* **79**, 2971 (1997).
 - [4] M. Shnürer, Z. Cheng, M. Hentschel, G. Tempea, P. Kálmán, T. Brabec, and F. Krausz, *Phys. Rev. Lett.* **83**, 722 (1999).
 - [5] K. J. Schafer and K. C. Kulander, *Phys. Rev. Lett.* **78**, 638 (1997).
 - [6] D. G. Lee, H. J. Shin, Y. H. Cha, K. H. Hong, J. H. Kim, and C. H. Nam, *Phys. Rev. A* **63**, 021801(R) (2001).
 - [7] J. B. Watson, A. Sanpera, and K. Burnett, *Phys. Rev. A* **51**, 1458 (1995).
 - [8] C. Kan, C. E. Capjack, R. Rankin, and N. H. Burnett, *Phys. Rev. A* **52**, R4336 (1995).
 - [9] H. J. Shin, D. G. Lee, Y. H. Cha, K. H. Hong, and C. H. Nam, *Phys. Rev. Lett.* **83**, 2544 (1999); H. J. Shin, D. G. Lee, Y. H. Cha, J. H. Kim, K. H. Hong, and C. H. Nam, *Phys. Rev. A* **63**, 053407 (2001).
 - [10] J. H. Kim, H. J. Shin, D. G. Lee, and C. H. Nam, *Phys. Rev. A* **62**, 055402 (2000).
 - [11] M. B. Gaarde, F. Salin, E. Constant, Ph. Balcou, K. J. Schafer, K. C. Kulander, and A. L'Huillier, *Phys. Rev. A* **59**, 1367 (1999).
 - [12] Ph. Balcou, A. S. Dederichs, M. B. Gaarde, and A. L'Huillier, *J. Phys. B* **32**, 2973 (1999).
 - [13] E. Yablonovitch, *Phys. Rev. A* **10**, 1888 (1974).
 - [14] S. C. Wilks, J. M. Dawson, and W. B. Mori, *Phys. Rev. Lett.* **61**, 337 (1988).
 - [15] Wm. M. Wood, C. W. Siders, and M. C. Downer, *Phys. Rev. Lett.* **67**, 3523 (1991).

- [16] S. C. Rae and K. Burnett, Phys. Rev. A **46**, 1084 (1992).
- [17] P. Chessa, E. De Wispelaere, F. Dorchies, V. Malka, J. R. Marquès, G. Hamoniaux, P. Mora, and F. Amiranoff, Phys. Rev. Lett. **82**, 552 (1999).
- [18] J. H. Kim, D. G. Lee, H. J. Shin, and C. H. Nam, Phys. Rev. A **63**, 063403 (2001).
- [19] M. V. Ammosov, N. B. Delone, and V. P. Krainov, Sov. Phys. JETP **64**, 1191 (1986).
- [20] A. E. Siegman, *Lasers* (Oxford University Press, Oxford, 1986).
- [21] P. Salières, Ph. Antoine, A. de Bohan, and M. Lewenstein, Phys. Rev. Lett. **81**, 5544 (1998).
- [22] The laser pulse experienced by atoms in the case of Fig. 3(b) resembles in form that used in our previous discussions on the coherent sum method [10] and the time-frequency analysis [18]. Thus, the slope of the Wigner distributions shown in Figs. 4(b) and 5(b) gives the dynamic chirp.
- [23] C. Altucci, C. Delfin, L. Roos, M. B. Gaarde, A. L'Huillier, I. Mercer, T. Starczewski, and C. G. Wahlström, Phys. Rev. A **58**, 3934 (1998).
- [24] T. Sekikawa, T. Ohno, T. Yamazaki, Y. Nabekawa, and S. Watanabe, Phys. Rev. Lett. **83**, 2564 (1999).

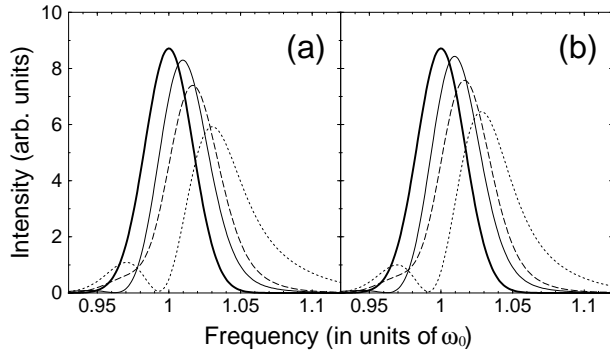


FIG. 1. (a) Laser spectra obtained from Eq. (2) for a 30-fs (FWHM) laser pulse of wavelength $\lambda = 800$ nm after propagating through a Ne gas medium of length $l = 700 \mu\text{m}$. The laser intensity and gas density are given by $I = 1 \times 10^{15} \text{ W/cm}^2$ and $N_0 = 1 \times 10^{18} \text{ cm}^{-3}$ ($\simeq 28$ Torr) (thin solid line); $I = 1 \times 10^{15} \text{ W/cm}^2$ and $N_0 = 3 \times 10^{18} \text{ cm}^{-3}$ ($\simeq 85$ Torr) (dotted line); $I = 3 \times 10^{15} \text{ W/cm}^2$ and $N_0 = 1 \times 10^{18} \text{ cm}^{-3}$ (dashed line). The spectrum of the incident laser pulse is drawn by a thick solid line. (b) Laser spectra obtained by direct numerical calculations of Eq. (1) for the same parameters as in (a).

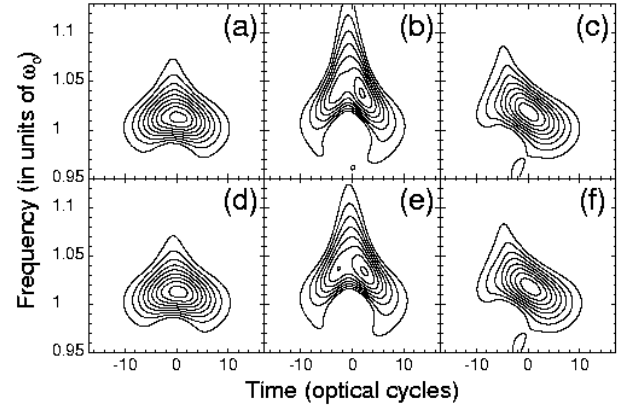


FIG. 2. Wigner distributions of the laser pulses specified in Fig. 1. In (a)-(c) [(d)-(f)], the same parameters are used as for the thin solid, dotted and dashed lines in Fig. 1(a) [Fig. 1(b)], respectively. Only positive contour lines are shown.

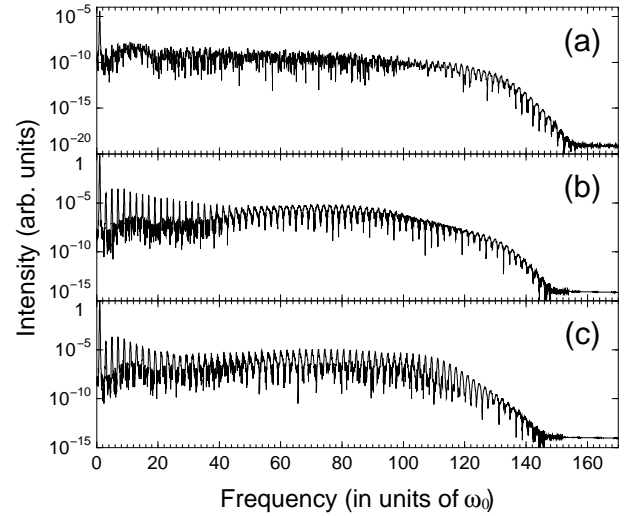


FIG. 3. (a) Single-atom harmonic spectrum for a Ne atom placed at the entrance of the medium. (b) Macroscopic harmonic spectrum (in the far field, on the axis) considering only the effect of laser focusing. (c) Macroscopic harmonic spectrum taking into account both the focusing and plasma effects. A Ne gas medium of density $N_0 = 1 \times 10^{18} \text{ cm}^{-3}$ and length $l = 700 \mu\text{m}$ is irradiated by a 30-fs (FWHM) Gaussian laser pulse of wavelength $\lambda = 800$ nm. The medium is centered at $x = 2$ mm behind the focus, and because of focusing ($b = 4$ mm) the laser intensity decreases from $I = 1 \times 10^{15} \text{ W/cm}^2$ at the entrance to $I = 0.7 \times 10^{15} \text{ W/cm}^2$ at the exit of the medium.

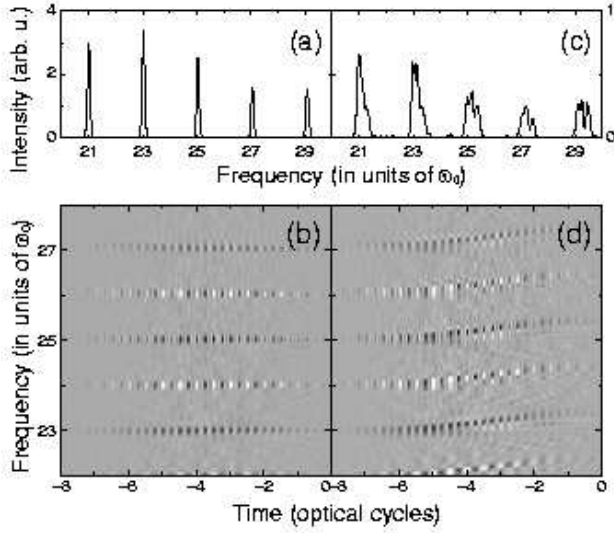


FIG. 4. (a) Enlarged view (on a linear scale) of Fig. 3(b) between $20\omega_0$ and $30\omega_0$ (only the focusing effect is considered). (b) Wigner distribution of the harmonics chosen in (a). (c) [(d)] Same as (a) [(b)] except that harmonics are chosen from Fig. 3(c) (both the focusing and plasma effects are considered). Positive and negative values of the Wigner distribution are colored black and white, respectively.

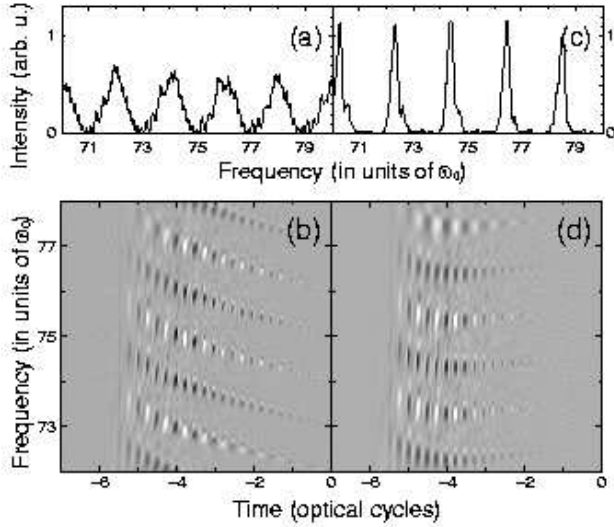


FIG. 5. Same as Fig. 4 except that harmonics between $70\omega_0$ and $80\omega_0$ are chosen here.